

First-Principles Estimation of Electronic Temperature from X-Ray Thomson Scattering Spectrum of Isochorically Heated Warm Dense Matter

Chongjie Mo,^{1,2} Zhenguo Fu,³ Wei Kang,^{1,4,5,*} Ping Zhang,^{1,3,5,†} and X. T. He^{1,3,5,‡}


¹HEDPS, Center for Applied Physics and Technology, Peking University, Beijing 100871, China

²School of Physics, Peking University, Beijing 100871, China

³Institute of Applied Physics and Computational Mathematics, Beijing 100088, China

⁴College of Engineering, Peking University, Beijing 100871, China

⁵Collaborative Innovation Center of IFSA (CICIFSA), Shanghai Jiao Tong University, Shanghai 200240, China

 (Received 2 August 2017; revised manuscript received 24 March 2018; published 18 May 2018)

Through the perturbation formula of time-dependent density functional theory broadly employed in the calculation of solids, we provide a first-principles calculation of x-ray Thomson scattering spectrum of isochorically heated aluminum foil, as considered in the experiments of Sperling *et al.* [*Phys. Rev. Lett.* **115**, 115001 (2015)], where ions were constrained near their lattice positions. From the calculated spectra, we find that the electronic temperature cannot exceed 2 eV, much smaller than the previous estimation of 6 eV via the detailed balance relation. Our results may well be an indication of unique electronic properties of warm dense matter, which can be further illustrated by future experiments. The lower electronic temperature predicted partially relieves the concern on the heating of x-ray free electron laser to the sample when used in structure measurement.

DOI: [10.1103/PhysRevLett.120.205002](https://doi.org/10.1103/PhysRevLett.120.205002)

A warm dense state of a material is broadly concerned in inertial confinement fusion [1–4], planetary physics [5], and laboratory astrophysics [6]. Owing to the development of experimental techniques, especially the advent of x-ray free electron lasers (XFELs) [7], high-power lasers [8,9], and Z apparatus [10], the difficulty of generating a warm dense state under laboratory conditions is much relieved. Instead, the description of the state, including both experimental diagnosis [11–14] and theoretical modeling [15–17], is emerging as a focus of the investigation. This inquiry has motivated and strongly supported the development of several diagnostic techniques, e.g., the streaked optical pyrometers [18,19], the x-ray absorption spectra [12,13,16], and in parallel, the x-ray Thomson scattering (XRTS) methods [11,20], all of which are closely related to the detection of electronic transitions in warm dense matter (WDM).

The XRTS method is viewed as a promising technique to measure internal properties of WDM [20]. Comprehensive information of the material, including that of electronic structures, ion structures, thermal properties, and transport properties, etc., are conveyed in the XRTS spectra. This prospect has been greatly strengthened recently by the progress of XRTS experiments [11,21–23], especially by their impressive accuracy and resolution in the measurement of scattering spectra. However, extracting material properties from measured XRTS spectra remains a grand theoretical challenge. This situation is similar to or even worse than that in the x-ray absorption experiments. The underlying difficulties are attributed to the complex

dependency of XRTS spectra on material parameters, such as temperature, density, and even the degree of a WDM system apart from its equilibrium state.

As long as the XRTS method considered as a diagnostic tool, the measurement of electronic temperature T_e can serve as a critical calibration reference, and thus has attracted much attention recently [11,22,24,25]. In addition, measuring T_e itself is also of fundamental interest to WDM. It is not only essential to the determination of the equation of state, but is also a prerequisite to the understanding of the electron-ion energy transfer process in materials under the exposure of a high-power laser [26].

It is usually difficult to extract a single condition parameter such as T_e from the XRTS spectra without knowing other parameters. The recent isochoric heating technique [11] of XFELs, however, greatly reduces the complicity of determining T_e . With the motion of ions suppressed by their own inertia in the short heating period of several femtoseconds, the influence of ions on electronic transitions is approximately a stationary value. The only undetermined parameter left in the system is T_e , provided that electrons are in equilibrium with each other, as usually assumed in WDM experiments [27]. A recent forward XRTS experiment [11] on isochorically heated warm dense aluminum (Al) is such an excellent example (with so far the most accurate measurements) that theoretical interpretation of the XRTS spectra can be conducted under well-controlled conditions.

In this Letter, we provide a first-principles estimation of T_e based on the experimental XRTS spectra measured by

Sperling *et al.* [11]. In the first-principles method, ion-electron interactions and the major part of electron-electron interactions are self-consistently included at the density functional theory (DFT) level [28]. The scattering of electrons in the x-ray electric field are taken into account by the time-dependent density functional theory (TDDFT) with a linear response perturbation formula [29]. Our calculations display that T_e of the warm dense Al cannot exceed 2 eV. It is much smaller than the previous estimation of 6 eV via the detailed balance relation [11], which may not be reliable as expected because the method is extremely sensitive to small fluctuations in measuring the spectrum strength [30]. Our results may well indicate the unique electronic properties of WDM, which can be further demonstrated by future experiments and theories. The lower T_e predicted can partially relieve the concern of XFELs in heating the sample as a structure measurement tool [31].

We focus on the inelastic scattering of x-ray photons by electrons in the Al foil, as considered by the experiment [11]. Direct scattering from ions is neglected because the cross section is inversely proportional to the square of the mass of charged particles [32]. To keep a close comparison with the experimental results, we follow the experimental way [33] to decompose the intensity $I(\mathbf{q}, \omega)$ of the scattered x ray at the transferred momentum \mathbf{q} and the transferred energy ω into two parts as

$$I(\mathbf{q}, \omega) \propto |f_c(\mathbf{q}) + \rho(\mathbf{q})|^2 S_{ii}(\mathbf{q}, \omega) + Z S_{ee}(\mathbf{q}, \omega), \quad (1)$$

with $f_c(\mathbf{q})$ as the form factor of the core (bound) electrons, $\rho(\mathbf{q})$ as the form factor of the screening electrons, S_{ii} as the ion-ion dynamic structure factor, Z as the number of valence (unbound) electrons, and S_{ee} as the dynamic structure factor of valence electrons. The atomic units together with $k_B = 1$ will be used hereinafter in the formulas.

The first part in Eq. (1) represents the quasielastic scattering. As has been revealed by experiments [33], it only corresponds to a sharp peak at the origin point of ω with its width being much smaller than the experimental resolution. So, it can be treated as a Dirac delta function without missing the major feature of the scattering spectrum [33]. The second part represents the scattering associated with electronic transitions. It can be calculated from the electronic density response function $\chi_{ee}(\mathbf{q}, \omega)$ through the fluctuation-dissipation theorem as [20]

$$S_{ee}(\mathbf{q}, \omega) = \left(\frac{-1}{1 - \exp(-\omega/T_e)} \right) \text{Im} \left(\frac{\chi_{ee}(\mathbf{q}, \omega)}{\pi n_e} \right), \quad (2)$$

where n_e is the electronic charge density.

It has been well recognized [20,32] that $\chi_{ee}(\mathbf{q}, \omega)$ and thus $S_{ee}(\mathbf{q}, \omega)$ in WDM should be calculated through quantum-mechanical formulas. However, even in the same

theoretical framework, there are various choices to carry out the calculation. Usually the calculation of χ_{ee} in plasmas starts from free electrons [20], in which the $\chi_{ee}(\mathbf{q}, \omega)$ is first evaluated perturbatively at the random phase approximation (RPA) level. The contribution from electron-ion and electron-electron interactions, i.e., collisions in the interaction picture, is then added through the Mermin's collisional frequency approximation [34–37], the local field approximation [37–39], or a combination of both.

Instead, one can start the calculation from DFT calculations, which has been prevalently employed in condensed matter systems and WDM systems. In this method, the electronic wave functions are calculated by the Mermin's finite temperature version of the DFT [28], which takes into account the majority of electron-electron and electron-ion interactions. The $\chi_{ee}(\mathbf{q}, \omega)$ and $S_{ee}(\mathbf{q}, \omega)$ can then be calculated at the RPA level or using the TDDFT [29,40,41] to go beyond RPA, and the perturbation formula proposed by Petersilka *et al.* [29] is adopted in our work. The finite temperature effect [42,43] to the exchange-correlation functional is not considered due to its small effect around the solid density of Al [44,45]. The effect might be more noticeable at a lower density as suggested by Karasiev *et al.* [44]. Compared with the calculation starting from free electrons, the DFT-based approach avoids empirical models as much as possible and theoretically is more transparent.

In perturbation formulas, the $\chi_{ee}(\mathbf{q}, \omega)$ is the Fourier transformation of the density response function $\chi_{ee}(\mathbf{r}, \mathbf{r}')$ in real space, which is the solution of a Dyson-like equation [29]

$$\chi_{ee}(\mathbf{r}, \mathbf{r}', \omega) = \chi_{ee}^0(\mathbf{r}, \mathbf{r}', \omega) + \int d\mathbf{r}_1 d\mathbf{r}_2 \chi_{ee}^0(\mathbf{r}, \mathbf{r}_1, \omega) \times K(\mathbf{r}_1, \mathbf{r}_2, \omega) \chi_{ee}(\mathbf{r}_2, \mathbf{r}', \omega), \quad (3)$$

with $K(\mathbf{r}_1, \mathbf{r}_2, \omega) = 1/|\mathbf{r}_1 - \mathbf{r}_2| + f_{xc}^{\text{TD}}(\mathbf{r}_1, \mathbf{r}_2, \omega)$. Here f_{xc}^{TD} is the time-dependent exchange-correlation kernel. When f_{xc}^{TD} is set to be zero, Eq. (3) goes back to the RPA formula of χ_{ee} . χ_{ee}^0 is the bare density response function, which can be written as the summation of all contributions of electronic transitions as

$$\chi_{ee}^0(\mathbf{r}, \mathbf{r}', \omega) = \sum_{j \neq k} (f_k - f_j) \frac{\phi_k(\mathbf{r}) \phi_j^*(\mathbf{r}') \phi_j(\mathbf{r}) \phi_k^*(\mathbf{r}')}{\omega - (\epsilon_j - \epsilon_k) + i\eta}, \quad (4)$$

where f_i is the Fermi-Dirac occupation of the i th level, ϕ_i is the corresponding wave function, and η is the Lorentzian broadening factor. The readers are referred to Ref. [29] for details of the method. Recent calculations of Timrov *et al.* [41] on Al at room temperature displayed that this method had a very good accuracy for the scattering at $|\mathbf{q}| \sim 0.8 \text{ bohr}^{-1}$ when the adiabatic local density approximation

(ALDA) for f_{xc} and an appropriate constant η is used. It is therefore employed in our calculations. In further developments, one can go beyond the treatment of η as a constant following Cazzaniga *et al.* [46] by taking the energy-dependent η into consideration, which will lead to a much broader application range of the TDDFT method. In principle, $\chi_{ee}(\mathbf{q}, \omega)$ contains all contributions from core and valence electrons. However, the transitions from the core electrons, i.e., those in the K and L shells, are larger than 70 eV [47], which is beyond the energy range of $|\omega| < 50$ eV probed by the experiment [11]. So, the calculations can be further simplified by only explicitly including the three valence electrons using the pseudopotential technique. Note that core levels at T_e of several electron volts are fully occupied, and transitions between them are thus suppressed. The concern of a mixture of transitions between valence electrons and those between core electrons in S_{ee} does not occur at this low T_e regime. But when T_e increases further, this mixture will be important and has to be carefully treated, as pointed out by Baczewski *et al.* [40].

In the calculations, 32 Al ions are fixed to the face-centered-cubic (fcc) lattice with a lattice parameter $a = 7.653$ bohr. Wave functions are generated using the FT-DFT calculation with the local density approximation (LDA) at the given electronic temperature T_e . A $3 \times 3 \times 3$ unshifted k -point mesh is used to resolve the Brillouin zone. The effective ion-electron interaction is represented by a normal conserving pseudopotential with three valence electrons. An energy cutoff of 80 Ry and 1600 energy bands are used to ensure the convergence of wave functions.

In the calculation of $\chi_{ee}(\mathbf{q}, \omega)$ and $S_{ee}(\mathbf{q}, \omega)$ with the TDDFT method, the resolution of ω is 0.1 eV. The ALDA of f_{xc} is adopted in the calculation following Ref. [41]. To compensate the effect of finite sampling in the Brillouin zone, a Gaussian smearing factor of 1.0 eV is also used to smooth the spectrum. The transferred momentum is set to be $|\mathbf{q}| = 0.890$ bohr $^{-1}$, corresponding to the scattering angle of 24° at the x-ray energy of 7980 eV used in the experiment.

For comparison purposes, we also calculate S_{ee} of molten Al in random structures with $T_i = T_e$. In these cases, the ionic configurations are generated with a Γ -point first-principles molecular dynamics (FPMD) simulation at the given temperature, with a time step of 1 fs. The ionic trajectories in the last 1 ps are saved for the calculation of S_{ee} described above, after the system reaches its equilibrium. Each presented spectrum of S_{ee} is the average of eight snapshots of the ionic configurations uniformly selected from the saved equilibrium ionic trajectories.

The FPMD and DFT calculations are carried out using the QUANTUM ESPRESSO package [48], and the $\chi_{ee}(\mathbf{q}, \omega)$ and $S_{ee}(\mathbf{q}, \omega)$ are calculated using the YAMBO code [49]. The accuracy and reliability of our method are carefully examined with previous results. Details are summarized in the Supplemental Material [50].

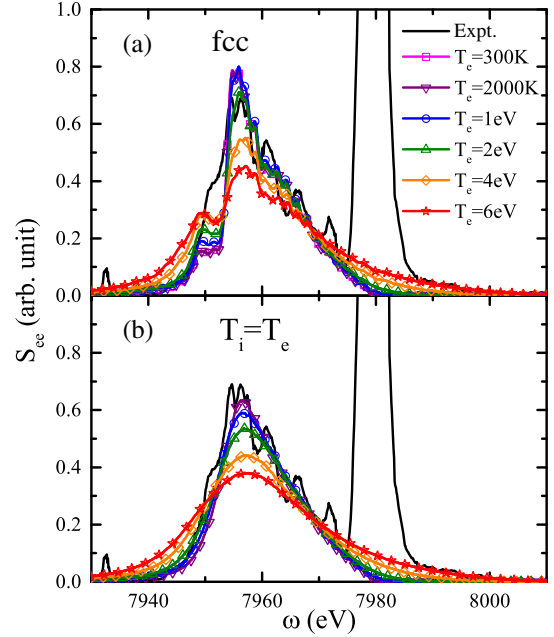


FIG. 1. Calculated S_{ee} together with deconvolved XRTS spectrum measured by Sperling *et al.* [11]. (a) The TDDFT results in a fcc Al lattice at T_e ranging from 300 K to 6 eV, calculated with $\eta = 0.1$ eV. (b) The TDDFT results in molten Al at $T_i = T_e$ from 1 to 6 eV. Note that in (a) the S_{ee} for $T_e = 300$ and 2000 K are almost identical.

Figure 1(a) displays the temperature dependence of S_{ee} , where the origin point of ω is shifted to 7980 eV in order to compare with the experimental measurements. The spectra are calculated at $|\mathbf{q}| = 0.890$ bohr $^{-1}$ in the fixed fcc lattice. The deconvolved experimental spectrum is also displayed in the figure as black dashed lines. All spectra are normalized with the sum rule of $\int_{-\infty}^{\infty} d\omega \omega S_{ee}(\mathbf{q}, \omega) = q^2/2$ [53,54]. The S_{ee} in Fig. 1(a) demonstrates typical features of a plasmonic peak. It shows that the maximum of the peak at around 7955 eV is not sensitive to the temperature variation. However, with the increasing of T_e , the height of the peak decreases and the tail at low energy gets more weights. Consequently, the FWHM of the peak increases. It is noticeable that the $S_{ee}(\omega)$ at $T_e > 2$ eV has a distinguishable difference from the experimental spectrum.

In the experiments, ions may deviate from the lattice position randomly for various reasons, although these deviations might be small. For example, the randomness can be caused by the polycrystalline structure of the Al foil or by the heating of the incident x-ray laser. Figure 1(b) considers the condition that ions are in equilibrium with electrons, i.e., $T_i = T_e$, which represents the extreme case that the randomness of ions have a maximum influence on $S_{ee}(\omega)$. However, Fig. 1(b) shows that the randomness of ions can only smooth out the subtle features of the spectra and slightly lower the height of the plasmonic peak by less than 10%. This suggests that the randomness of ions does

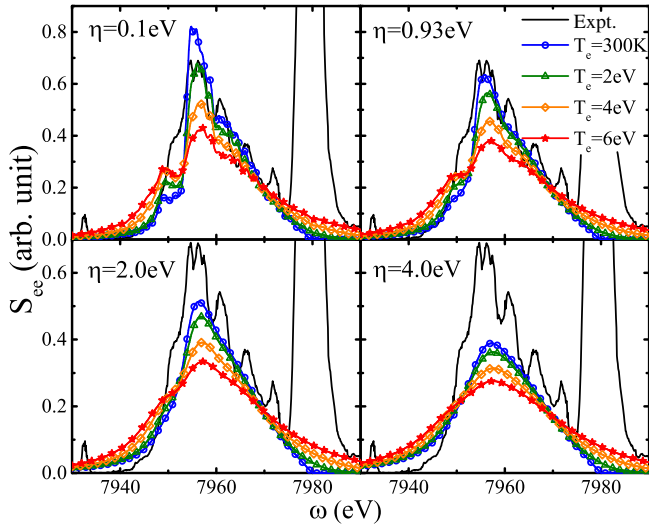


FIG. 2. Calculated S_{ee} using the TDDFT method with η from 0.1 to 4.0 eV. In each case, S_{ee} calculated at $T_e = 300$ K, 2 eV, 4 eV, and 6 eV are compared.

not have a remarkable influence on $S_{ee}(\omega)$, and the best fit of $S_{ee}(\omega)$ should be located somewhere between the results of crystalline structure and the melted structure [55]. In addition, the randomness of ions slightly increases the difference between the calculated S_{ee} and the measured spectrum when $T_e \geq 1$ eV. This further suggests that the T_e corresponding to the measured S_{ee} cannot be much larger than 2 eV.

Influences of Lorentzian broadening factor η are examined in Fig. 2 for $T_e = 300$ K, 2 eV, 4 eV, and 6 eV. Physically, the factor η in Eq. (4) is associated with the lifetime τ of excitations as $\tau \sim (2\eta)^{-1}$ according to the uncertainty principle. In the figure, η covers the range from 0.1 to 4.0 eV, corresponding to τ from 0.5 to 20 fs. In each case, the profile of the spectra becomes flattened with the increasing of η . This tendency is in line with the general expectation of line broadening of a Lorentzian type. However, the figure displays that only the calculations with η from 0.1 to 1 eV at low temperatures are comparable with the measurement. When $\eta > 2.0$ eV or $T_e > 2.0$ eV, none of the calculations can reproduce the experimental spectrum. On the other hand, the η cannot be much smaller than 0.1 eV because the x-ray pulse length is 25 fs, corresponding to $\eta \sim 0.08$ eV. So, the results essentially imply that T_e should be not greater than 2 eV in order to reproduce the experimental results no matter how one adjusts the η [57].

To give further support to our results, we also compare the experimental S_{ee} with the measurement of Cazzaniga *et al.* [46] at room temperature, as displayed in Fig. 3. The S_{ee} of Cazzaniga *et al.* was measured with synchrotron radiation at $|\mathbf{q}| = 0.821$ bohr $^{-1}$, which is quite close to the one ($|\mathbf{q}| = 0.890$ bohr $^{-1}$) we are interested in. Also displayed are our calculations at $T_e = 300$ K, where η is set to

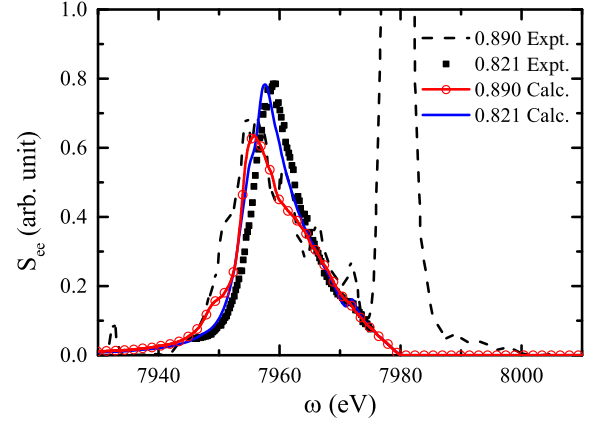


FIG. 3. Comparison between the S_{ee} in the experiment of Sperling *et al.* [11] at $|\mathbf{q}| = 0.890$ bohr $^{-1}$ with the measurement of Cazzaniga *et al.* [46] at $|\mathbf{q}| = 0.821$ bohr $^{-1}$. The latter experiment was performed at room temperature. Also displayed are corresponding TDDFT calculations at $T_e = 300$ K.

be 0.93 eV, the same as that used in Ref. [41]. It is not surprising to see that the two spectra are similar because the two $|\mathbf{q}|$'s are close to each other. In particular, both have a sharp decay around 7950 eV. This feature is quite different from that in the spectra displayed in Fig. 1(a) for $T_e > 2$ eV, which have a slowly decaying tail in the low-energy part. In addition, Fig. 3 shows that the calculated spectra at the same T_e (300 K) describe the features of both measurements well, suggesting that the T_e 's of these two S_{ee} 's are quite close.

Figure 4 shows the influence of the instrument function, which was also measured by Sperling *et al.* in the same experiment. Although some of the detailed features of S_{ee} are smoothed out by convoluting the spectra with the

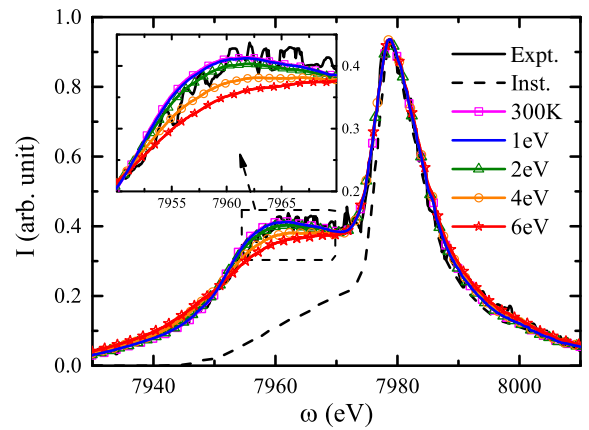


FIG. 4. Calculated S_{ee} with the responses (the instrument function) of the apparatus taken into account, compared with the measured spectrum of Sperling *et al.* [11]. Results presented are calculated by convoluting the S_{ee} in Fig. 1 with the instrument function measured in the experiment [11], which is displayed as dashed lines.

instrument function, the figure shows that the experimental result can only be reproduced with T_e not larger than 2 eV. When T_e increases further, the deviation between the calculated spectra and the measurement becomes appreciable. Therefore, the effective T_e in the experiment of Sperling *et al.* would not exceed 2 eV at best, when compared with the calculations.

In summary, through systematic TDDFT calculations, we find that T_e is not larger than 2 eV in the XRTS experiment of Sperling *et al.*, much smaller than the 6 eV estimated based on a less reliable method. Our results may well reflect the unique electronic properties and transitions in WDM. However, to arrive at that conclusion, a reliable estimation of T_e from XRTS is necessary. Other methods, e.g., estimating T_e from the shift of the K -absorption edge [16], may help to further examine this issue. In addition, the lower T_e predicted relieves, at least partially, the concern to the heating of the sample of XFEL as a structure measurement tool [31].

This work is financially supported by the Science Challenge Project No. TZ2016001, the NSAF (Grants No. U1530113 and No. U1530258) and the NSFC (Grants No. 11675023, No. 11274019, and No. 11275032). Part of the calculations are supported by the Special Program for Applied Research on Super Computation of the NSFC-Guangdong Joint Fund (the second phase) under Grant No. U1501501.

*weikang@pku.edu.cn

†zhang_ping@iapcm.ac.cn

‡xthe@iapcm.ac.cn

- [1] J. Lindl, *Phys. Plasmas* **2**, 3933 (1995).
- [2] X. He, J. Li, Z. Fan, L. Wang, J. Liu, K. Lan, J. Wu, and W. Ye, *Phys. Plasmas* **23**, 082706 (2016).
- [3] S. E. Bodner, D. G. Colombant, J. H. Gardner, R. H. Lehmberg, S. P. Obenschain, L. Phillips, A. J. Schmitt, J. D. Sethian, R. L. McCrory, W. Seka *et al.*, *Phys. Plasmas* **5**, 1901 (1998).
- [4] E. Campbell, V. Goncharov, T. Sangster, S. Regan, P. Radha, R. Betti, J. Myatt, D. Froula, M. Rosenberg, I. Igumenshchev *et al.*, *Matter Radiat. Extremes* **2**, 37 (2017).
- [5] T. Guillot, *Science* **286**, 72 (1999).
- [6] B. A. Remington, R. P. Drake, and D. D. Ryutov, *Rev. Mod. Phys.* **78**, 755 (2006).
- [7] Y. Ding, A. Brachmann, F.-J. Decker, D. Dowell, P. Emma, J. Frisch, S. Gilevich, G. Hays, P. Hering, Z. Huang *et al.*, *Phys. Rev. Lett.* **102**, 254801 (2009).
- [8] J. Soares, S. Loucks, and R. McCrory, *Fusion Sci. Technol.* **30**, 492 (1996).
- [9] X. He and W. Zhang, *Eur. Phys. J. D* **44**, 227 (2007).
- [10] M. K. Matzen, M. Sweeney, R. Adams, J. Asay, J. Bailey, G. Bennett, D. Bliss, D. Bloomquist, T. Brunner, R. B. Campbell *et al.*, *Phys. Plasmas* **12**, 055503 (2005).
- [11] P. Sperling, E. J. Gamboa, H. J. Lee, H. K. Chung, E. Galtier, Y. Omarbakiyeva, H. Reinholz, G. Röpke, U. Zastra, J. Hastings, L. B. Fletcher, and S. H. Glenzer, *Phys. Rev. Lett.* **115**, 115001 (2015).
- [12] Y. Zhao, J. Yang, J. Zhang, G. Yang, M. Wei, G. Xiong, T. Song, Z. Zhang, L. Bao, B. Deng *et al.*, *Phys. Rev. Lett.* **111**, 155003 (2013).
- [13] A. Benuzzi-Mounaix, F. Dorchie, V. Recoules, F. Festa, O. Peyrusse, A. Levy, A. Ravasio, T. Hall, M. Koenig, N. Amadou, E. Brambrink, and S. Mazevet, *Phys. Rev. Lett.* **107**, 165006 (2011).
- [14] S. Vinko, O. Ciricosta, B. Cho, K. Engelhorn, H.-K. Chung, C. Brown, T. Burian, J. Chalupský, R. Falcone, C. Graves *et al.*, *Nature (London)* **482**, 59 (2012).
- [15] G. Gregori, S. H. Glenzer, W. Rozmus, R. W. Lee, and O. L. Landen, *Phys. Rev. E* **67**, 026412 (2003).
- [16] S. Zhang, S. Zhao, W. Kang, P. Zhang, and X.-T. He, *Phys. Rev. B* **93**, 115114 (2016).
- [17] S. Vinko, O. Ciricosta, and J. Wark, *Nat. Commun.* **5** (2014).
- [18] J. E. Miller, T. R. Boehly, A. Melchior, D. D. Meyerhofer, P. M. Celliers, J. H. Eggert, D. G. Hicks, C. M. Sorce, J. A. Oertel, and P. M. Emmel, *Rev. Sci. Instrum.* **78**, 034903 (2007).
- [19] Z. Chen, L. Hao, W. Zhebin, J. Xiaohua, Z. Huige, L. Yonggang, L. Zhichao, L. Sanwei, Y. Dong, D. Yongkun *et al.*, *Plasma Sci. Technol.* **16**, 571 (2014).
- [20] S. H. Glenzer and R. Redmer, *Rev. Mod. Phys.* **81**, 1625 (2009).
- [21] U. Zastra, P. Sperling, M. Harmand, A. Becker, T. Bornath, R. Bredow, S. Dziarzhytski, T. Fennel, L. Fletcher, E. Förster *et al.*, *Phys. Rev. Lett.* **112**, 105002 (2014).
- [22] L. Fletcher, H. Lee, T. Döppner, E. Galtier, B. Nagler, P. Heimann, C. Fortmann, S. LePape, T. Ma, M. Millot *et al.*, *Nat. Photonics* **9**, 274 (2015).
- [23] P. Davis, T. Döppner, J. Rygg, C. Fortmann, L. Divol, A. Pak, L. Fletcher, A. Becker, B. Holst, P. Sperling *et al.*, *Nat. Commun.* **7**, 11189 (2016).
- [24] K. Falk, E. J. Gamboa, G. Kagan, D. S. Montgomery, B. Srinivasan, P. Tzeferacos, and J. F. Benage, *Phys. Rev. Lett.* **112**, 155003 (2014).
- [25] L. Fletcher, A. Kritcher, A. Pak, T. Ma, T. Döppner, C. Fortmann, L. Divol, O. Jones, O. Landen, H. Scott *et al.*, *Phys. Rev. Lett.* **112**, 145004 (2014).
- [26] B. Cho, T. Ogitsu, K. Engelhorn, A. Correa, Y. Ping, J. Lee, L. Bae, D. Prendergast, R. Falcone, and P. Heimann, *Sci. Rep.* **6**, 18843 (2016).
- [27] R. P. Drake, *High-Energy-Density Physics: Fundamentals, Inertial Fusion, and Experimental Astrophysics* (Springer Science & Business Media, Berlin, 2006).
- [28] N. D. Mermin, *Phys. Rev.* **137A**, 1441 (1965).
- [29] M. Petersilka, U. J. Gossmann, and E. K. U. Gross, *Phys. Rev. Lett.* **76**, 1212 (1996).
- [30] See Sec. S1 of the Supplemental Material at <http://link.aps.org/supplemental/10.1103/PhysRevLett.120.205002> for the influence of fluctuations.
- [31] R. A. Valenza and G. T. Seidler, *Phys. Rev. B* **93**, 115135 (2016).
- [32] W. Schülke, *Electron Dynamics by Inelastic X-Ray Scattering* (Oxford University, Oxford, 2007).
- [33] E. G. Saiz, G. Gregori, D. O. Gericke, J. Vorberger, B. Barbrel, R. Clarke, R. R. Freeman, S. Glenzer, F. Khattak, M. Koenig *et al.*, *Nat. Phys.* **4**, 940 (2008).

- [34] N. D. Mermin, *Phys. Rev. B* **1**, 2362 (1970).
- [35] H. Reinholz, R. Redmer, G. Röpke, and A. Wierling, *Phys. Rev. E* **62**, 5648 (2000).
- [36] H. Reinholz, *Ann. Phys. (Paris, Fr.)* **30**, 1 (2005).
- [37] Z.-G. Fu, Z. Wang, M.-L. Li, D.-F. Li, W. Kang, and P. Zhang, *Phys. Rev. E* **94**, 063203 (2016).
- [38] M. D. Barriga-Carrasco, *Phys. Rev. E* **79**, 027401 (2009).
- [39] C. Fortmann, A. Wierling, and G. Röpke, *Phys. Rev. E* **81**, 026405 (2010).
- [40] A. D. Baczewski, L. Shulenburger, M. P. Desjarlais, S. B. Hansen, and R. J. Magyar, *Phys. Rev. Lett.* **116**, 115004 (2016).
- [41] I. Timrov, N. Vast, R. Gebauer, and S. Baroni, *Phys. Rev. B* **88**, 064301 (2013).
- [42] E. W. Brown, B. K. Clark, J. L. DuBois, and D. M. Ceperley, *Phys. Rev. Lett.* **110**, 146405 (2013).
- [43] V. V. Karasiev, T. Sjostrom, J. Dufty, and S. B. Trickey, *Phys. Rev. Lett.* **112**, 076403 (2014).
- [44] V. V. Karasiev, L. Calderin, and S. B. Trickey, *Phys. Rev. E* **93**, 063207 (2016).
- [45] S. Zhang, H. Wang, W. Kang, P. Zhang, and X. T. He, *Phys. Plasmas* **23**, 042707 (2016).
- [46] M. Cazzaniga, H.-C. Weissker, S. Huotari, T. Pylkkänen, P. Salvestrini, G. Monaco, G. Onida, and L. Reining, *Phys. Rev. B* **84**, 075109 (2011).
- [47] R. D. Deslattes, E. G. Kessler, P. Indelicato, L. de Billy, E. Lindroth, and J. Anton, *Rev. Mod. Phys.* **75**, 35 (2003).
- [48] P. Giannozzi, S. Baroni, N. Bonini, M. Calandra, R. Car, C. Cavazzoni, D. Ceresoli, G. L. Chiarotti, M. Cococcioni, I. Dabo *et al.*, *J. Phys. Condens. Matter* **21**, 395502 (2009).
- [49] A. Marini, C. Hogan, M. Grning, and D. Varsano, *Comput. Phys. Commun.* **180**, 1392 (2009).
- [50] See Supplemental Material at <http://link.aps.org/supplemental/10.1103/PhysRevLett.120.205002> for details of the examination, which includes Refs. [51, 52].
- [51] G. Onida, L. Reining, and A. Rubio, *Rev. Mod. Phys.* **74**, 601 (2002).
- [52] H. J. Monkhorst and J. D. Pack, *Phys. Rev. B* **13**, 5188 (1976).
- [53] See Supplemental Material at <http://link.aps.org/supplemental/10.1103/PhysRevLett.120.205002> for details of the normalization.
- [54] G. D. Mahan, *Many-Particle Physics* (Kluwer Academic, New York, 2000).
- [55] Details of the best fit of $S_{ee}(\omega)$ and influences of numerical fluctuations are provided in Sec. S5 of the Supplemental Material at <http://link.aps.org/supplemental/10.1103/PhysRevLett.120.205002>, which includes Ref. [56].
- [56] R. Verbeni, T. Pylkkänen, S. Huotari, L. Simonelli, G. Vanko, K. Martel, C. Henriquet, and G. Monaco, *J. Synchrotron Radiat.* **16**, 469 (2009).
- [57] See the Supplemental Material at <http://link.aps.org/supplemental/10.1103/PhysRevLett.120.205002> for the comparison with original measured XRTS signal.